

Algal biofuel: bountiful lipid from *Chlorococcum* sp. proliferating in municipal wastewater

Durga Madhab Mahapatra^{1,2} and T. V. Ramachandra^{1,2,3,*}

¹Energy and Wetlands Research Group, Centre for Ecological Sciences, ²Centre for Sustainable Technologies, and

³Centre for Infrastructure, Sustainable Transport and Urban Planning, Indian Institute of Science, Bangalore 560 012, India

Algae biofuel have emerged as viable renewable energy sources and are the potential alternatives to fossil-based fuels in recent times. Algae have the potential to generate significant quantities of commercially viable biofuel apart from treating wastewater. Three algal species, viz. *Chlorococcum* sp., *Microcystis* sp. and *Phormidium* sp. proliferating in wastewater ponds were isolated and cultured in the laboratory myxotrophically under similar wastewater conditions. *Chlorococcum* sp. attained a mean biomass productivity of $0.09 \text{ g l}^{-1} \text{ d}^{-1}$ with the maximum biomass density of 1.33 g l^{-1} and comparatively higher lipid content of 30.55% (w/w) on the ninth day of the culture experiment. Under similar conditions *Microcystis* sp. and *Phormidium* sp. attained mean biomass productivities of 0.058 and $0.063 \text{ g l}^{-1} \text{ d}^{-1}$ with a total lipid content of 8.88% and 18.66% respectively. Biochemical composition (carbohydrates, proteins, lipids and phosphates) variations and lipid accumulation studies were performed by comparison of the ratios of carbohydrate to protein; lipid to protein (L/P) and lipid to phosphates using attenuated total reflectance-Fourier transform infrared spectroscopy which showed higher L/P ratio during the stationary phase of algal growth. Composition analysis of fatty acid methyl ester has been performed using gas chromatography and mass spectrometry. *Chlorococcum* sp. with higher productivity and faster growth rate has higher lipid content with about 67% of saturated fatty acid dominated by palmitate (36.3%) followed by an unsaturate as linoleate (14%) and has proved to be an economical and viable feedstock for biofuel production compared to the other wastewater-grown species.

Keywords. Algae, biofuel, fatty acid, lipid, wastewater.

ENERGY plays a pivotal role in the economic and social development of a region or a nation. The hydrocarbon-based fossil fuels with the share of 45% in the total energy needs are the key economic driver in India¹ and are getting exhausted at alarming rates². Escalating energy prices coupled with the fast dwindling stock has necessitated substitution for fossil fuels. In this context,

algal biofuels while providing clean energy, also help in the mitigation of greenhouse gases (GHGs) and aptly have become the focus of research in recent times^{3,4}. Studies reveal that algal species like *Chlorella* sp.⁵ and *Scenedesmus* sp.^{6,7} have higher growth rates, while *Botryococcus brauni*⁸ and *Dunaliella tertiolecta*⁹ are efficient in storing lipids in the form of triacylglycerides (TAGs).

Growing algae for biofuel can be one of the sustainable options of harvesting solar energy optimally. Nutrients from wastewater and atmospheric carbon dioxide produce useful lipids in algae. These algae aid as an interface between the atmosphere and hydrosphere, similar to solar panels in manifesting the incident solar energy into biochemical energy, which is stored as lipids³. Addition of nutrients into the water would stimulate the algal growth, but this entails cost for fertilizing the water that would eventually lower the net benefit in terms of cost and also reduce the total energy gain in the system. Wastewater generated in enormous amounts¹⁰ from human habitations could ensure sustained growth of algae and biofuel generation^{11,12}. The use of wastewater for algal biofuel production would ensure sustainability in terms of (a) biofuel production, (b) nutrient removal and remediation of wastewater and (c) mitigation of GHGs. Thus the development of renewable clean algal biofuel fosters sustainability and helps in maintaining the environment quality.

Screening and scrutiny of efficient algal species are necessary for assessing the biofuel prospects of algae¹³. Especially the native or indigenous algal species thriving in the wastewater conditions with at high N and P (refs 14 and 15) concentration would be more beneficial than the commercially available strains which have a narrow range of tolerance. The locally isolated algae easily adapt to the wastewater conditions and are found to grow at higher biomass densities^{11,14}. Fourier transform infrared (FTIR) spectroscopy helps in rapid determination of lipids and identification of target algae by the unique spectral signatures (characteristic of each algal species) and this constitutes an easy and accurate method to assess lipid accumulation and quantification¹¹. In the present study algae growth rate, biomass density, productivity and lipid content of the select wastewater algae have been

*For correspondence. (e-mail: cestvr@ces.iisc.ernet.in)

investigated. FTIR spectroscopy was used for the determination of characteristic spectral signatures of each algae. The transitions in the proteins, carbohydrates, lipids and phosphates were also monitored across the growth period. Lipids were extracted and fatty acid methyl ester (FAME) profiling was carried out using gas chromatography and mass spectrometry (GC-MS).

The objectives of the present study are (i) To determine the lipid content with fatty acid (FAME) composition and biomass productivity of the algal species grown profusely in wastewater. (ii) To identify the spectral signatures and study the cellular compositional changes in wastewater-grown algae with the culture time. (iii) To identify the potential algal species growing in wastewater, suitable for sustainable biofuel production.

Materials and methods

Collection of wastewater algae

Algae growing in wastewater were collected from sewage-fed freshwater lakes (Bellandur and Varthur, Bangalore South) of Bangalore and sewage treatment plant (Rayan kere sewage treatment plant (STP)) at Mysore, Karnataka, India. Samples were collected during the mid-day as algal densities are expected to be higher at peak photosynthetic period in such open waters. Water samples were also collected for laboratory analysis.

Isolation and culturing

Water samples (200 ml) containing algae were centrifuged (5000 rpm) repeatedly and washed with deionized water. The near-pure populations of select algae were then serially diluted and spread over nutrient agar plates. After growth in agar plates, they were inoculated in 500 ml Erlenmeyer flask containing artificial wastewater medium prepared according to Yujie *et al.*¹⁶ and incubated at 25°C under cool white fluorescent light (~4000 lux) and a light to dark period of 16:8 h was maintained. The monitoring of algal growth was carried out through an optical microscope every two days. Identification, enumeration and counting of algal samples were done using standard keys and protocols^{17,18}. Isolated microalgae were then concentrated to a cell density of 10⁷ cells/ml and inoculated to filtered-sterilized wastewater¹⁹ (collected from STP). Later algae were cultivated in batch mode for 10 days in 1 litre. Erlenmeyer flasks with a working volume of 1 litre. Every day the algal cells were harvested, centrifuged and were checked for growth and compositional variability, and were dried at 60°C for dry weight measurements. All experiments were conducted in triplicate; the data presented are expressed as mean ± SD ($\mu \pm SD$). The physico-chemical parameters and nutrients in the wastewater used for culturing are provided in Table 1.

Table 1. Physico-chemical characteristics of domestic wastewater used for the experiments

| Physico-chemical parameters | Values |
|---|--------------|
| pH | 6.9 ± 0.1 |
| Redox potential (ORP; mV) | -107 ± 26 |
| Total solids (TS; mg l ⁻¹) | 1360 ± 78 |
| Total suspended solids (TSS; mg l ⁻¹) | 518 ± 61 |
| Total volatile solids (TVS; mg l ⁻¹) | 278 ± 34 |
| Total nitrogen (TN; mg l ⁻¹) | 38 ± 2.86 |
| Ammonium-nitrogen (NH ₄ -N; mg l ⁻¹) | 31 ± 4.62 |
| Nitrate-nitrogen (NO ₃ -N; mg l ⁻¹) | 0.13 ± 0.077 |
| Nitrite-nitrogen (NO ₂ -N; mg l ⁻¹) | 0.04 ± 0.018 |
| Total phosphorus (TP; mg l ⁻¹) | 19.5 ± 3.24 |
| Ortho-phosphates (OP; mg l ⁻¹) | 17 ± 2.77 |
| Total organic carbon (TOC; mg l ⁻¹) | 193 ± 16 |
| Chemical oxygen demand (COD; mg l ⁻¹) | 470 ± 47 |

Lipid extraction

The total lipids content was determined according to Bligh and Dyer²⁰. The cell disruption was performed by ultra-sonication (frequency 35 kHz) for 30 min in continuous mode at 25°C, the lipids were extracted with chloroform-methanol (2:1, v/v) and then separated into chloroform and aqueous methanol layers by the addition of methanol and water to give a final solvent ratio of chloroform: methanol: water as 2:1.1:0.9. The chloroform layer was then evaporated using a rotary vacuum evaporator with a water bath temperature of 60°C and lipids were concentrated.

Lipid extraction and processing

Lipid classes were separated through one-dimensional thin-layer chromatography (TLC) using TLC plates (10 × 10 cm, 0.25 mm thickness, Merck, Darmstadt, Germany) coated with silica gel. The solvent system used for elution of lipids was a combination of petroleum ether: diethyl ether: acetic acid in a ratio of 70:30:1 (mobile phase; v/v). The bands were visualized after staining the TLC plates with iodine vapour according to standard TLC protocols. The TAG layer was carefully removed and collected immediately and was processed for lipid extraction. The presence of lipid compounds was detected by brown bands against a white background, which were compared with the coconut oil standard.

Spectral signatures and biochemical composition transition by ATR-FTIR

Composition of algal biomass and the type of functional groups of the algal extract are assessed through FTIR spectroscopy study. Attenuated total reflectance (ATR)-FTIR spectra were collected on a Bruker Alpha Spec Instrument. Dried algal cells were pressed against the

diamond cell prior to scanning. The extracts from *Chlorococcum* sp., *Microcystis* sp. and *Phormidium* sp. with coconut oil (standard) were observed for their functionalities in the spectrogram. The spectra were collected in the mid-IR range (64 scans) from 4000 to 800 cm^{-1} (at a spectral resolution of 2 cm^{-1}) and data were analysed using Origin Pro 8 SR0, v8.0724 (B724) with an initial baseline correction and scaled up to amide I_{max} . The peaks with each of the spectral curves were carefully fitted and calculated²¹. The biochemical transitions in the algal cells were monitored by the analysis of carbohydrate to protein (C/P), lipid to protein (L/P) and lipid to phosphate (L/Phos.) ratios^{22–24}.

Analysis of fatty acid methyl ester profile

Methylation of lipids was performed by converting all fatty acids to their corresponding methyl esters (transesterification) using boron trifluoride–methanol ($\text{BF}_3\text{-MeOH}$) and H_2SO_4 as catalyst. $\text{BF}_3\text{-MeOH}$ converts fatty acids to their methyl esters and has been used as the most common catalyst for FAME preparation. The extracted samples were heated at 60°C for 15 min. They were then cooled in an ice-bath for 5 min followed by the addition of 1 ml water and hexane respectively. After settling, the top hexane layer was removed and washed using anhydrous sodium sulphate for further purification. The methylated sample was loaded onto silica column with helium gas as carrier in splitless mode. The total run time was calculated to be 47.667 min. Fatty acids were identified by comparing the retention time obtained to that of known standards. The composition of FAME was assessed through gas chromatograph (Agilent Technologies 7890C, GC System) with detection by mass spectrometry (Agilent Technologies 5975C insert mass selective detector (MSD) with triple-axis detector). HP-5% phenyl methyl siloxane: 756-42744 column was used; maximum temperature 325°C and column dimensions 30 m \times 250 μm \times 0.25 μm that was purged with helium gas.

The injection and detector temperatures were maintained at 250°C and 280°C respectively (ASTM D 2800). One microlitre volume of sample was injected into the column, whose initial temperature was maintained at 40°C. After 1 min, the oven temperature was raised to 100°C at a ramp rate of 10°C min^{-1} . It was further raised to 150°C at a ramp rate of 2°C min^{-1} ; then to 230°C at a ramp rate of 3°C min^{-1} and finally to 300°C at a ramp rate of 10°C min^{-1} ; this temperature was maintained for 2 min. The components were identified based on their retention times, abundance and fragmentation patterns.

Results and discussion

Algae grow at a faster rate with the ability to accumulate substantial quantities of lipid²⁵. In the present study the

algae isolated from wastewater were selected on the basis of their predominance in wastewater across seasons. There have been many studies for screening of oleaginous algae¹³ that are being isolated and characterized under controlled and outdoor culture conditions⁵. These algae grow copiously²⁵ with adequate nutrient supply and under suitable conditions.

The peak growth of *Chlorococcum* sp. occurred on the 8th day, indicating enhanced growth rate corresponding to the time of incubation. Similarly, *Microcystis* sp. reached its peak growth on the fourth day and *Phormidium* sp. on the sixth day, indicating lack of lag phase. This indicates their capability to acclimatize wastewater conditions and grow exponentially during the 9-days growth experiment. Figure 1 illustrates the growth curve of the selected algae from wastewater. Biomass density (dry wt. g l^{-1}) of *Chlorococcum* sp. ($1.33 \pm 0.072 \text{ g l}^{-1}$) is about 1.69 times higher than *Microcystis* sp. ($0.78 \pm 0.059 \text{ g l}^{-1}$) and about 1.43 times higher than *Phormidium* sp. ($0.93 \pm 0.073 \text{ g l}^{-1}$). However, longer growth period was observed in case of *Chlorococcum* sp. compared to the other two species. The specific growth rate (SGR) was higher during the initial period, i.e. first three days of the culture experiment (Figure 2). *Chlorococcum* sp. attained the highest SGR of 0.75 d^{-1} , with a mean of 0.161 d^{-1} . *Microcystis* sp. achieved the highest SGR of 0.68 d^{-1} with a mean of 0.122 d^{-1} . In the case of *Phormidium* sp.,

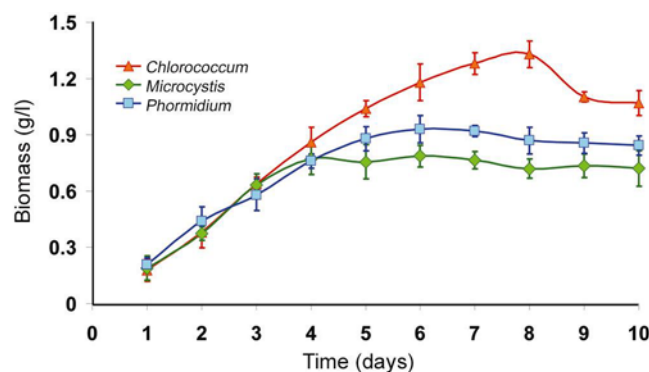


Figure 1. Growth curves of algal species.

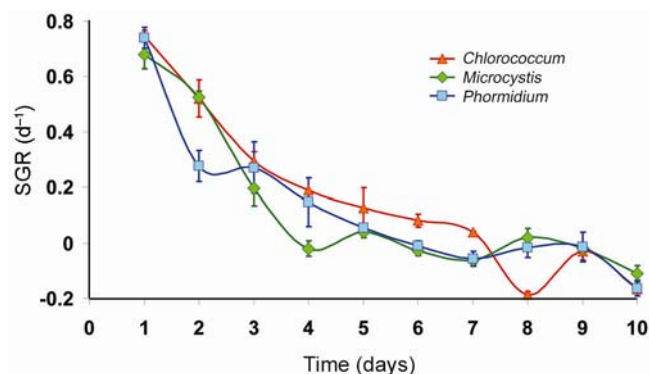


Figure 2. Variation in the specific growth rate (SGR) per day of the algal species.

the highest SGR was observed to be 0.74 d^{-1} with a mean of 0.123 d^{-1} . *Chlorococcum* sp. attained a mean biomass productivity of $0.09 \text{ g l}^{-1} \text{ d}^{-1}$ during the culture experiment. Under similar conditions, *Microcystis* sp. and *Phormidium* sp. attained a biomass productivity of 0.064 and $0.072 \text{ g l}^{-1} \text{ d}^{-1}$ respectively.

After the exponential growth period, the algal species were harvested and biomass used for oil extraction. Among the isolated algal species, *Chlorococcum* sp. showed the highest lipid content of $30.55 \pm 2.65\%$. *Microcystis* sp. showed the lowest lipid content of $8.88 \pm 1.78\%$ and *Phormidium* sp. showed a moderate lipid content of $18.66 \pm 2.34\%$, albeit producing a higher biomass in the initial phases. Under stressful environments or during unfavourable conditions, algae tend to slow down their cell division and quickly utilize available carbon for synthesizing high energy density compounds like lipids to combat or adjust to nutrient limiting conditions^{7,22}. In the present study increased lipid accumulation has been observed during the stationary stages of growth, which is in accordance with the earlier studies⁸. N limitation results in lower photosynthetic C fixation for proteins synthesis evident from the carbohydrate to amide ratio (discussed later), consequently stocking carbon in the form of lipids or carbohydrates, depending on the species¹¹.

The lipid content reported earlier is in the range 20–50% (refs. 25 and 26), however some oleaginous algae can have very high lipid content > 70% (ref. 8). Growth of *Auxenchlorella protothecoides* in concentrated sewage showed a lipid accumulation of 32% (ref. 19). Similarly, 30% lipid accumulation was observed in *Scenedesmus* sp. growing in secondary wastewater⁵. Studies on green algae growing in dairy and municipal wastewaters showed a maximum lipid content of 29% (ref. 27). Studies on *Chlorella vulgaris* grown in artificial wastewater showed a higher lipid accumulation of 37% (ref. 5).

Numerous studies have used techniques like chromatography and fluorescent stains like NILE RED for determining lipid accumulation²⁸, but these methods have disadvantages in terms of time and cost for processing, accuracy, etc. Analysis through FTIR is much easier and advantageous for the measurement of biochemical composition of algal cells and lipid accumulation studies. A number of studies have reported good correlation of the composition through the measurement of band intensities, when compared with advanced methods^{21,29}. Many algal species have been analysed using FTIR spectroscopy for compositional quantification, including *Chaetoceros muellerii*²²; *Pediastrum* sp.³⁰; *Scenedesmus* sp., *Phormidium* sp., *Nitzschia* sp. and *Sphaerocystis* sp.²⁹; *Microcystis aeruginosa*, *Croococcus minutus*, *Nostoc* sp., *Cyclotella meneghiniana* and *Phaeodactylum tricoratum*²¹; *Chlamydomonas reinhardtii* and *Scenedesmus subspicatus*⁷ and *Dunaliella tertiolecta* and *Thalassiosira pseudonana*³¹.

The ATR-FTIR characteristic spectral signatures ($4000\text{--}400 \text{ cm}^{-1}$) of lipids from algal species *Chlorococcum* sp., *Microcystis* sp. and *Phormidium* sp. compared with the standard coconut oil are elucidated in Figure 3. The absorption bands in the FTIR spectrum are indicative of the presence of hydroxyl (–OH), carbonyl (C=O), aromatic C, alkane, alkene and amide groups in the algal species. The bands at 3299 , 3345 and 3279 cm^{-1} are due to the O–H stretching vibrations in the algal species. However, no prominent bands were observed in the standard lipid due to absence of OH species (Figure 3, top). A weak band with a small peak at 2923 cm^{-1} can be attributed to asymmetric C–H vibrations, mostly due to methylene groups of lipids (Figures 3 and 4). The bands noticed at 2855 cm^{-1} are assigned to symmetric C–H vibrations in *Chlorococcum* sp. and other species, due to stretching of methyl groups of lipids. The bands at 2338 cm^{-1} correspond to CO_2 vibrations. The prominent bands present $\sim 1740\text{--}1640 \text{ cm}^{-1}$ are due to the presence of C=O of esters or fatty acids (Figure 4). The bands following these C=O peaks are the amide I and amide II mostly present in 1630 and 1574 cm^{-1} , due to the presence of C=O groups on proteins, C≡N bonds and C–H, N–H associated with proteins respectively. A small band at 1240 cm^{-1} can be assigned to P=O stretch by the phospho-diester backbone present in nucleic acids (DNA and RNA). A prominent band at $\sim 1000 \text{ cm}^{-1}$ in the studied algal species is due to the C–O–C stretching in polysaccharides. Few small bands found $\sim 800\text{--}550 \text{ cm}^{-1}$ are attributed to aromatic C–H bending. The characteristic lipid peak can be distinctively visualized in the coconut oil standard FTIR spectra at $\sim 1700 \text{ cm}^{-1}$ (Figure 4; top). The FTIR spectra of *Chlorococcum* sp. with different band assignments from 4000 to 400 cm^{-1} are depicted in Figure 4.

The ATR-FTIR spectra of the selected algal cell showed 7 distinct absorption bands from the wavenumbers ranging from 1800 to 800 cm^{-1} (Table 2). These bands were assigned to specific functional groups following biochemical standards and published literature²¹. The assignments of bands corresponding to the functional groups are provided in Table 2. Four bands were most important for the study, i.e. $\sim 1740 \text{ cm}^{-1}$ for ester/fatty acid, $\sim 1655 \text{ cm}^{-1}$ for proteins, $\sim 1240 \text{ cm}^{-1}$ for phosphates and $\sim 1150\text{--}950 \text{ cm}^{-1}$ for carbohydrates (Figure 4). FTIR spectrogram of the algal species has a specific spectral signature in terms of lipids and other biochemical compositions, and indeed has a different fingerprint for lipids in *Chlorococcum* sp. and the two other algal species. Figure 5 a–c illustrates the changes in the FTIR spectra with the culture time from day 1 to day 10 for *Chlorococcum* sp., *Microcystis* sp. and *Phormidium* sp. respectively and the macromolecular compositions are depicted in Table 3. The compositional changes were monitored by the carbohydrate/amide (C/P), lipid/amide (L/P) and lipid/phosphate (L/Phos.) changes of algal species as depicted in Figure 6 a–c. The cultures experienced

an increase in L/P ratio. The FTIR assignments of bands to the spectra in case of the three selected algae showed significant variation in the carbohydrate, protein, lipid and phosphate contents (Figure 5).

The C/P ratio showed a peak on the day 6th of the culture in the case of *Microcystis* sp. and day 8th of the culture in case of *Phormidium* sp. (Figure 6a). This is indicative of the higher polysaccharide content in the biomass due to rapid total organic carbon (TOC) assimilation through heterotrophy¹¹ from the 2nd to 6th and 8th day in the

culture. The C/P ratio dropped consistently in *Chlorococcum* sp., indicating C transformation from carbohydrates to lipids (Table 3). The higher C/P ratio in the studies shows potential N limitations that would have triggered lipid synthesis. In the present experiment, the C/P ratio varied from 2.27 to 0.63 (3.6 fold decrease; 10th day) in *Chlorococcum* sp.; 2.73 to 4.69 (1.71 fold increase; 10th day) in *Microcystis* sp. and 4.14 to 7.36 (1.78 fold increase; 8th day) in *Phormidium* sp. respectively. These C/P ratios are comparable to the studies of Stehfest *et al.*²¹ during N deplete conditions. However, the reason for a decrease in the C/P ratio can be due to C degradation at the end of the growth phase. Studies on *P. tricornutum* under nutrient-sufficient and N-deplete conditions showed

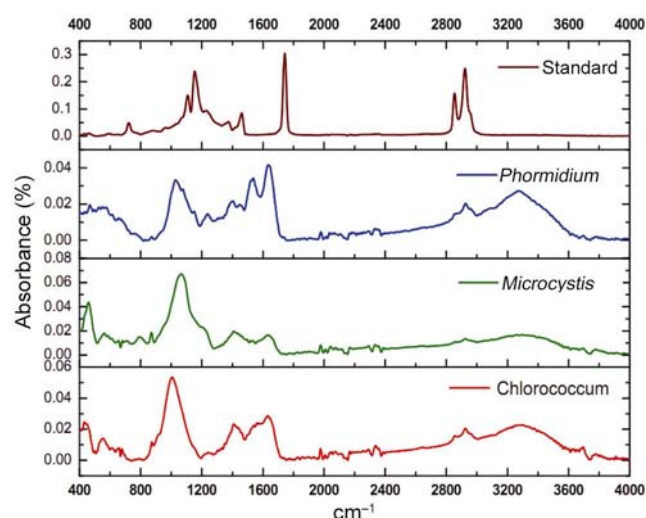


Figure 3. Comparative analysis of the Fourier transform infrared (FTIR) absorbance spectra of *Chlorococcum* sp., *Microcystis* sp., *Phormidium* sp. and lipid standard (coconut oil).

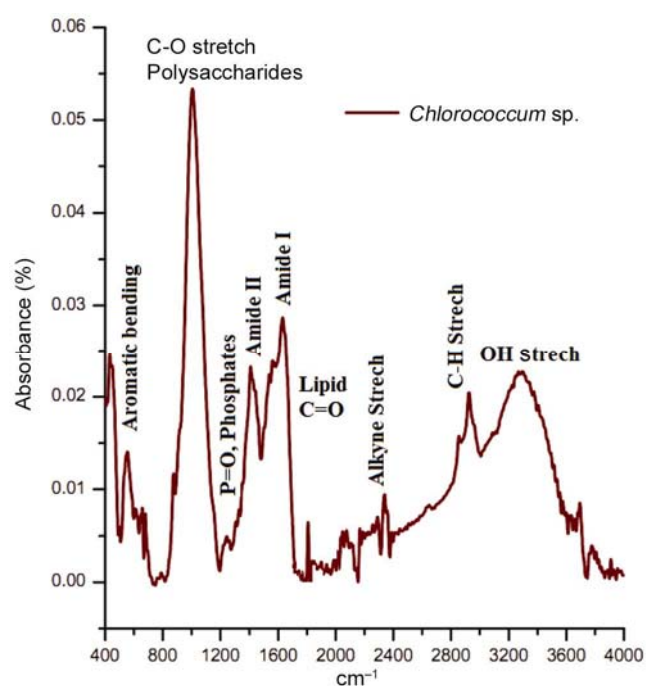


Figure 4. Attenuated total reflectance-FTIR spectra (mid-IR) of *Chlorococcum* sp. with specific bands assignments.

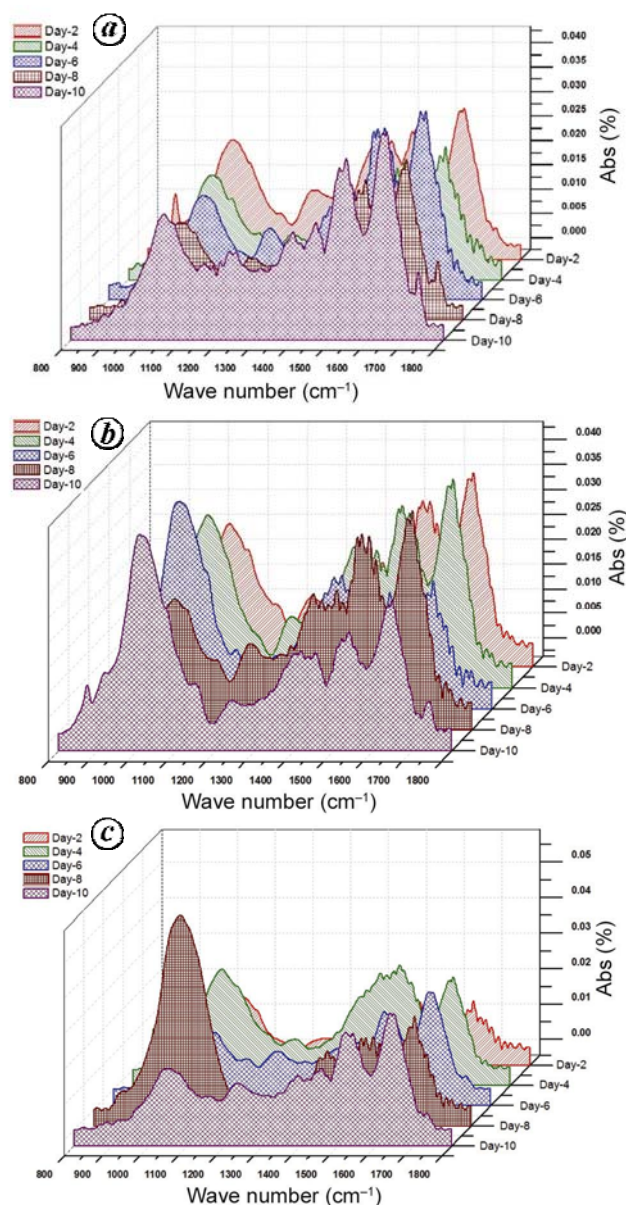


Figure 5. Transitions in the FTIR spectra of (a) *Chlorococcum* sp., (b) *Microcystis* sp. and (c) *Phormidium* sp. with culture time (10 days).

Table 2. FTIR band assignments for algal species

| Band assignments (cm ⁻¹) | Functional groups |
|---|--|
| ~ 1740 | $\nu(\text{C}=\text{O})$ stretching of ester groups, primarily from lipids and fatty acids |
| ~ 1655 | $\nu(\text{C}=\text{O})$ stretching of amides from proteins (amide I) |
| ~ 1545 | $\delta(\text{N}-\text{H})$ bending of amides from proteins (amide II) |
| ~ 1455 | $\delta_{\text{as}}(\text{CH}_2)$ and $\delta_{\text{as}}(\text{CH}_3)$ bending of methyl from proteins |
| ~ 1380 | $\delta_{\text{s}}(\text{CH}_2)$ and $\delta_{\text{s}}(\text{CH}_3)$ bending of methyl and $\nu_{\text{s}}(\text{C}-\text{O})$ stretching of COO- |
| ~ 1240 | $\nu_{\text{as}}(>\text{P}=\text{O})$ stretching, associated with phosphorus compounds |
| ~ 1000 | $\nu(\text{C}-\text{O}-\text{C})$ stretching from polysaccharides |

Table 3. Quantification of carbohydrates, proteins, lipids and phosphates (computed from area under the curve after deconvolution and peak fitting) with errors and the strength of the peak fitting (R^2)

| | Carbohydrates | Error | R^2 | Proteins | Error | R^2 | Lipids | Error | R^2 | Phosphates | Error | R^2 |
|---------------------|---------------|---------|---------|----------|----------|---------|---------|----------|---------|------------|---------|---------|
| <i>Chlorococcum</i> | | | | | | | | | | | | |
| Day-2 | 2.10273 | 0.02803 | 0.98729 | 0.92444 | 0.01324 | 0.99647 | 0.06905 | 0.00272 | 0.99247 | 0.09788 | 0.00469 | 0.89549 |
| Day-4 | 1.78347 | 0.03772 | 0.95792 | 0.74985 | 0.003872 | 0.95991 | 0.01886 | 0.00299 | 0.6647 | 0.04807 | 0.00245 | 0.91545 |
| Day-6 | 1.34877 | 0.01488 | 0.99226 | 1.05672 | 0.0172 | 0.98667 | 0.02601 | 0.00138 | 0.96425 | 0.20876 | 0.00952 | 0.97132 |
| Day-8 | 0.89808 | 0.01513 | 0.97318 | 0.98259 | 0.02026 | 0.99167 | 0.14777 | 0.01001 | 0.95981 | 0.01047 | 0.00487 | 0.86248 |
| Day-10 | 0.85444 | 0.0134 | 0.97332 | 1.33956 | 0.02661 | 0.99398 | 0.23361 | 0.00741 | 0.98496 | 0.17146 | 0.0051 | 0.93052 |
| <i>Microcystis</i> | | | | | | | | | | | | |
| Day-2 | 2.85779 | 0.7171 | 0.94563 | 1.04433 | 0.02154 | 0.99203 | 0.01193 | 0.00118 | 0.85977 | 0.08041 | 0.00326 | 0.95497 |
| Day-4 | 3.55536 | 0.03666 | 0.97658 | 1.20784 | 0.02833 | 0.9902 | 0.1199 | 0.0017 | 0.72852 | 0.04533 | 0.00114 | 0.97882 |
| Day-6 | 3.99281 | 0.07561 | 0.98286 | 0.60306 | 0.03448 | 0.93997 | 0.18686 | 0.12457 | 0.70767 | 0.01854 | 0.03509 | 0.86142 |
| Day-8 | 1.81889 | 0.5583 | 0.93714 | 1.0800 | 0.03099 | 0.98502 | 0.02142 | 0.00291 | 0.75282 | 0.11025 | 0.00301 | 0.9726 |
| Day-10 | 3.41205 | 0.04504 | 0.98243 | 0.72644 | 0.01592 | 0.98892 | 0.24735 | 0.02517 | 0.98114 | 0.02814 | 0.00203 | 0.94441 |
| <i>Phormidium</i> | | | | | | | | | | | | |
| Day-2 | 1.90205 | 0.02457 | 0.98611 | 0.45911 | 0.0369 | 0.88593 | 0.02249 | 0.00235 | 0.59866 | 1.4538 | 0.29058 | 0.98422 |
| Day-4 | 3.7678 | 0.08206 | 0.97325 | 1.47444 | 0.09348 | 0.96545 | 0.02923 | 0.006168 | 0.89853 | 0.28932 | 0.03793 | 0.97508 |
| Day-6 | 2.4166 | 0.05875 | 0.94139 | 1.722587 | 0.07604 | 0.98314 | 0.11465 | 0.00399 | 0.99431 | 0.31169 | 0.02535 | 0.95079 |
| Day-8 | 7.37841 | 0.05158 | 0.99471 | 1.00221 | 0.05831 | 0.9467 | 0.03635 | 0.00457 | 0.54673 | 0.25534 | 0.00976 | 0.97158 |
| Day-10 | 2.73937 | 0.06364 | 0.94218 | 2.02027 | 0.09046 | 0.98187 | 0.14962 | 0.00646 | 0.99172 | 0.18143 | 0.00688 | 0.89957 |

C/P ratio of 0.8 (1.14 fold increase; 14th day) and 0.3 (2.42 fold increase; 26th day) respectively however a 6.7 fold increase in *M. auregonosa* and 3.5 fold increase in *C. minutus* in C/P under N-deplete conditions was observed²¹. *C. reinhardtii* and *S. subspicatus* under lower N regimes showed a C/P ratio of 2.4 (9.6 fold increase; 10th day) and 1.5 (3.75 fold increase; 10th day) respectively⁷. Studies on *D. tertiolecta* and *T. pseudonana* showed a C/P ratio of 7.33 (2 fold increase; 5th day) and 17.6 (1.46 fold increase; 2nd day) in N-replete conditions respectively³¹. *Pediastrum duplex* under natural conditions showed an average C/P ratio of 0.6 (ref. 32).

There was clear increase in the L/P ratio towards the stationary phase (Figure 6b), which is due to a small increase in lipid with respect to proteins (Table 3). However in the case of *Microcystis* sp., there was a significant increase in the L/P ratio during the 6th day due to stationary phase of its growth and the highest L/P ratio (0.34) was observed on the 10th day. In case of *Chlorococcum* sp., the L/P ratio started picking up from the 6th day onwards. In case of *Phormidium* sp., the L/P variations were not significant ($P < 0.05$). In the present experiment, the

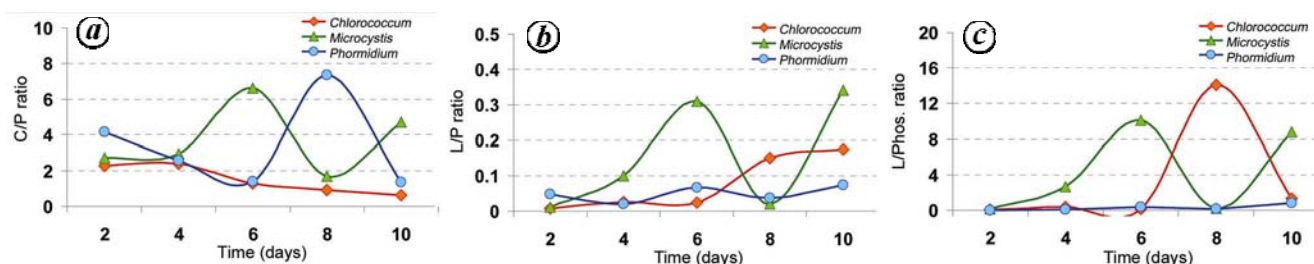
L/P ratio in case of *Chlorococcum* sp., *Microcystis* sp. and *Phormidium* sp. increased from 0.007 to 0.17 (24 fold increase; 10th day), 0.01 to 0.30 (30 fold increase; 6th day) and 0.04 to 0.07 (1.75 fold increase; 10th day) respectively, which is higher compared to the earlier studies^{21,32}. Studies on *P. tricornutum* under nutrient-sufficient conditions and N-deplete conditions showed L/P ratio of 0.23 (1.27 fold increase; 14th day) and 0.3 (1.2 fold increase; 26th day) respectively²¹. *C. reinhardtii* and *S. subspicatus* under lower N regimes showed L/P ratio of 1.4 (6.75 fold increase; 28th day) and 1.5 (7.1 fold increase; 15th day)⁷. Studies on *D. tertiolecta* and *T. pseudonana* showed a L/P ratio of 0.2 (5 fold increase; 6th day) and 0.63 (1.3 fold increase; 4th day) in N-deplete conditions respectively³¹. *P. duplex* under natural conditions showed an average L/P ratio of 0.2 (ref. 32).

The L/Phos. ratio increased on 6th and 8th day for *Microcystis* sp. and *Chlorococcum* sp. respectively (Figure 6c), which shows P limitation in the algae (Table 3). However, there was no significant variation between the L/Phos. ratio in *Phormidium* sp. Similar observations were also made by Jiang *et al.*³¹. In the present experiment, the

Table 4. Fatty acid composition of *Chlorococcum* sp., *Microcystis* sp., *Phormidium* sp. and standard coconut oil (% fatty acid methyl ester)

| C N : U | Fatty acyl methyl ester (%) | Standard | <i>Chlorococcum</i> | <i>Microcystis</i> | <i>Phormidium</i> |
|--|---|----------|---------------------|--------------------|-------------------|
| C 10 : 0 | Decanoic acid, methyl ester | 5.07 | – | – | – |
| C 11 : 0 | Undecanoic acid, methyl ester | – | 0.203 | – | – |
| C 12 : 0 | Dodecanoic acid, methyl ester | 46.49 | 1.016 | – | – |
| C 13 : 0 | Tridecanoic acid, methyl ester | – | 3.807 | 1.72 | 0.874 |
| C 14 : 0 | Methyl tetradecanoate | 22.45 | 13.117 | – | 4.214 |
| C 15 : 0 | Pentadecanoic acid, methyl ester | – | 9.916 | – | – |
| C 16 : 0 | Hexadecanoic acid, methyl ester | 9.17 | 36.124 | 46.34 | 64.194 |
| C 16 : 1(7) | 7-Hexadecenoic acid, methyl ester | – | 0.701 | – | 2.69 |
| C 16 : 1(9) | 9-Hexadecenoic acid, methyl ester | – | 3.565 | – | – |
| C 17 : 0 | Heptadecanoic acid, methyl ester | – | 0.449 | – | – |
| C 17 : 1(10) | cis-10-Heptadecenoic acid, methyl ester | – | 2.088 | – | – |
| C 18 : 0 | Octadecanoic acid, methyl ester | 7.94 | 6.322 | 7.11 | 5.522 |
| C 18 : 1(9) | 9-Octadecenoic acid, methyl ester | 7.23 | 1.592 | 6.54 | 1.56 |
| C 18 : 1(11) | 11-Octadecenoic acid, methyl ester | – | – | – | 3.455 |
| C 18 : 2(9,12) | 9,12-Octadecadienoic acid, methyl ester | 1.65 | 14.03 | 11.89 | 3.034 |
| C 18 : 3(9,12,15) | 9,12,15-Octadecatrienoic acid, methyl ester | – | 7.07 | 26.4 | 14.457 |
| Saturated fatty acids (saturates) | | 91.12 | 66.72 | 55.17 | 74.84 |
| Monoenoic fatty acids (mono-unsaturated fatty acids) | | 7.23 | 7.95 | 6.54 | 7.69 |
| Polyenoic fatty acids (Poly-unsaturated fatty acids) | | 1.65 | 21.1 | 38.29 | 17.49 |
| C16–C18 (fatty acids important: biodiesel perspective) | | 25.99 | 71.941 | 98.28 | 94.912 |
| Total lipid content | | | 30 | 8 | 18 |

–, Undetectable.

**Figure 6.** Changes in (a) carbohydrate/amide I (C/P) ratio, (b) lipid/amide I (L/P) ratio and (c) lipid/phosphate (L/Phos.) in the algal species.

L/Phos. ratio varied from 0.07 to 1.36 (19.4 fold increase; 10th day) in *Chlorococcum* sp., 0.14 to 8.78 (62 fold increase; 10th day) in *Microcystis* sp. and 0.01 to 0.82 (82 fold increase; 10th day) in *Phormidium* sp. respectively. Usually there is no change in phosphate content under N limitations and increase in the L/Phos. ratio can be as a result of increase in the lipid content in the cells. Studies on *P. tricornutum* under nutrient-sufficient and N-deplete conditions showed L/Phos. ratio of 0.25 (1.23 fold increase; 15th day) and 0.24 (1.2 fold increase; 14th day) respectively²¹. Studies on *D. tertiolecta* and *T. pseudonana* showed L/nucleic acid ratio of 0.4 (3 fold increase; 6th day) and 1.6 (1.6 fold increase; 8th day) in a combined growth set-up of N-replete and N-free media respectively³¹.

The FAME composition through GC-MS analysis showed 16 different types of fatty acid methyl esters, where most of them were saturated fatty acids (Table 4).

Palmitic acid (C16:0) is dominant with 36%, 46% and 64% in *Chlorococcum* sp., *Microcystis* sp. and *Phormidium* sp. respectively (Table 4). FAME studies showed higher percentage of saturated fatty acids (75%) in case of *Chlorococcum* sp., compared to unsaturated fatty acids in other algal species. The FAME chromatogram of *Chlorococcum* sp. is elucidated in Figure 7. The order of the major fatty acids in *Chlorococcum* sp. in the present study was C16:0 (~36%) > C18:2 (~14%) > C14:0 (~13%) > C15:0 (~9%) > C18:3 (~7%). However, in studies conducted by Harwati *et al.*³³ higher proportion of oleic acid C18:1 (~40%) was found and the order of major fatty acids was C18:1 (~40%) > C16:0 (~33%) > C18:2 (~11%) > C18:3 (~7%) > C18:0 (~6%). Higher C18:1 compared to C18:2 and C18:3 was observed in other studies^{34,35}. The FAME composition in the present study showed similar results as in case of *Chlorococcum humicola*, which was dominated by palmitate C16:0 and the

order of the major fatty acids found was C16:0 (~38%) > C18:3 (~18%) > C18:1 (~16%) > C18:2 (~13.5%) > C18:0 (~2%)³⁶. The studied FAME profile of the wastewater algal species showed similar composition to that of palm oil-based biodiesel. The oil containing higher percentages of C16 and C18 fatty acids provides a good balance for oxidation for longer storage³⁷ and a decreased cold filter plugging point to be used in cold places³⁸. Furthermore, the essential fatty acid from a biofuel perspective was found to be in higher percentages in all the three selected algae with 98.2%, 94.9% and 72% in *Microcystis* sp., *Phormidium* sp. and *Chlorococcum* sp. respectively (Table 4). Meagre quantities of polyunsaturated fatty acids were observed from the FAME analysis. Earlier studies³⁹ for checking the lipid class important from a biofuel point of view have showed C16–C18 as the most essential fatty acids having desirable biofuel properties. Palmitic, stearic, oleic and linolenic acids were recognized as the most common fatty acids contained in biodiesel⁴⁰.

Lipids with higher composition of palmitate and oleate show good biofuel properties such as quality ignition, higher oxidative stability and lubricity⁴⁰. Thus all selected wastewater algae were reasonably good from a biofuel point of view (Table 4) comprised of higher percentage of quality fatty acids for biofuel combustion. *Chlorococcum* sp. emerged best among the selected species due to

its higher growth rate, lipid content and good proportion of important fatty acids and can thus be used as a candidate from wastewater for energy generation and other combusive processes.

Conclusions

The present study highlights the capability of wastewater algae to grow at higher rates and with higher biomass productivity and store substantial amount of lipid. The highest growth ($1.33 \pm 0.072 \text{ g l}^{-1}$) was observed in *Chlorococcum* sp., that reached the stationary phase at the end of 9th day. The presence of lipid compounds and changes in biochemical macromolecular composition were verified with the help FTIR spectral analysis. Higher total lipid content was observed in *Chlorococcum* sp. that grows in wastewater ponds and lagoons. Palmitate was found out to be the most dominant among the FAME. Higher percentages of important fatty acids that are necessary from a biofuel combustion perspective is evident from FAME analysis. With higher lipid content, higher growth rate and desirable fatty acids content, *Chlorococcum* sp. stands out as an excellent candidate for biofuel/lipid production and can be used as a cheap option for sustainable biofuel production.

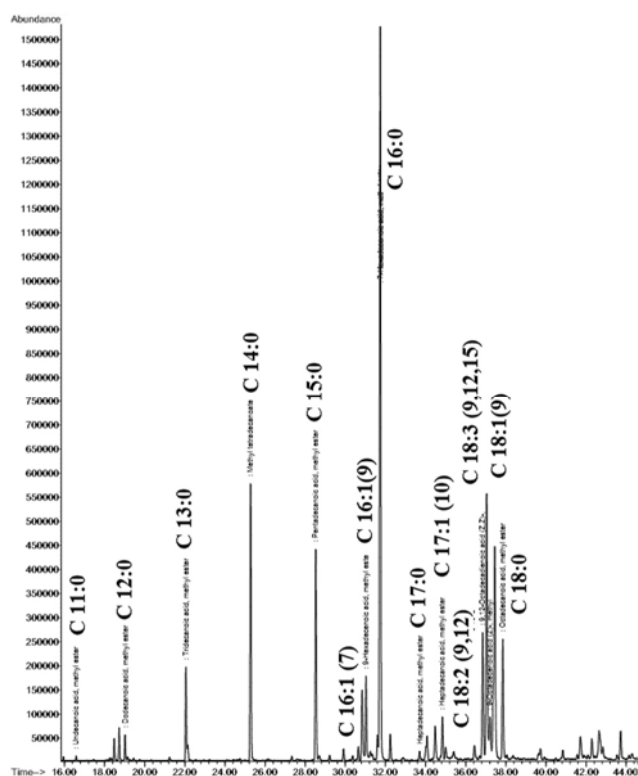


Figure 7. Fatty acid methyl ester composition of *Chlorococcum* sp. (gas chromatography and mass spectrometry).

1. Ministry of Petroleum and Natural Gas, Report of the Working Group on Petroleum and Natural Gas Sector, XI Plan (2007–2012); http://planningcommission.nic.in/aboutus/committee/wrk-grp11/wg11_petro.pdf (accessed on 4 October 2012).
2. Planning Commission. Government of India, Report of the Committee on Development of Bio-Fuel; http://planningcommission.nic.in/reports/genrep/cmtt_bio.pdf (accessed on 4 October 2012).
3. Ramachandra, T. V., Mahapatra, D. M., Karthick, B. and Gordon, R., Milking diatoms for sustainable energy: biochemical engineering vs gasoline secreting diatom solar panels. *Ind. Eng. Chem. Res.*, 2009, **48**, 8769–8788.
4. Chanakya, H. N., Mahapatra, D. M., Sarada, R. and Abitha, R., Algal biofuel production and mitigation potential in India. *Mitigat. Adaptat. Strateg. Global Change*, 2012, doi: 10.1007/s11027-012-9389z.
5. Feng, Y., Li, Chao and Zhang, D., Lipid production of *Chlorella vulgaris* cultured in artificial wastewater medium. *Bioresour. Technol.*, 2011, **101**, 101–105.
6. Li, X., Hu, H. Y., Gan, K. and Sun, Y. X., Effects of different nitrogen and phosphorus concentrations on the growth, nutrient uptake, and lipid accumulation of a freshwater microalga *Scenedesmus* sp. *Bioresour. Technol.*, 2010, **101**, 5494–5500.
7. Dean, A. P., Estrada, B., Sigee, D. C. and Pittman, J. K., Using FTIR spectroscopy for rapid determination of lipid accumulation in response to nitrogen limitation in freshwater microalgae. *Bioresour. Technol.*, 2010, **101**, 4499–4507.
8. Li, Y. and Qin, J. G., Comparison of growth and lipid content in three *Botryococcus braunii* strains. *J. Appl. Phycol.*, 2005, **17**, 551–556.
9. Takagi, M., Karseno and Yoshida, T., Effect of salt concentration on intracellular accumulation of lipids and triacylglyceride in marine microalgae *Dunaliella* cells. *J. Biosci. Bioeng.*, 2006, **101**, 223–226.
10. Mahapatra, D. M., Chanakya, H. N. and Ramachandra, T. V., Assessment of treatment capabilities of Varthur Lake, Bangalore. *Int. J. Environ., Technol. Manage.*, 2011, **14**, 84–102.

11. Mahapatra, D. M., Chanakya, H. N. and Ramachandra, T. V., *Euglena* sp. as a suitable source of lipids for potential use as bio-fuel and sustainable wastewater treatment. *J. Appl. Phycol.*, 2013, 1–11; doi: 10.1007/s10811-013-9979-5.
12. Prajapati, S. K., Kaushik, P., Malik, A. and Vijay, V. K., Phycoremediation and biogas potential of native algal isolates from soil and wastewater. *Bioresour. Technol.*, 2012, <http://dx.doi.org/10.1016/j.biortech.2012.08.069>
13. Sheehan, J., Dunahay, T., Benemann, J. and Roessler, P. G., US Department of Energy's Office of Fuels Development, A look back at the US Department of Energy's Aquatic Species Program Biodiesel from Algae. Close Out Report TP-580-24190. National Renewable Energy Laboratory, Golden, CO, USA, 1998.
14. Mahapatra, D. M., Chanakya, H. N. and Ramachandra, T. V., C : N ratio of sediments in a sewage fed urban lake. *Int. J. Geol.*, 2011, **5**, 86–92.
15. Mahapatra, D. M., Chanakya, H. N. and Ramachandra, T. V., Treatment efficacy of algae based sewage treatment plants. *Environ. Mon. Assess.*, 2013, 1–20; doi: 10.1007/s10661-013-3090-x.
16. Yujie, F., Li, C. and Zhang, D., Lipid production of *Chlorella vulgaris* cultured in artificial wastewater medium. *Bioresour. Technol.*, 2011, **102**, 101–105.
17. Prescott, G. W., *How to Know the Fresh Water Algae*, Cranbrook Press, Michigan, USA, 1959, vol. 1.
18. Desikacharya, T. V., *Cyanophyta*, ICAR, New Delhi, 1959, p 686.
19. Zhou, W., Min, M., Hu, B., Ma, X., Cheng, Y. and Chen, P., A hetero-photoautotrophic two-stage cultivation process to improve wastewater nutrient removal and enhance algal lipid accumulation. *Bioresour. Technol.*, 2012, **110**, 448–455.
20. Bligh, E. G. and Dyer, W. J., A rapid method of total lipid extraction and purification. *Can. J. Biochem. Physiol.*, 1959, **37**, 911–917.
21. Stehfest, K., Toepel, J. and Wilhelm, C., The application of micro-FTIR spectroscopy to analyse nutrient stress-related changes in biomass composition of phytoplankton algae. *Plant Physiol. Biochem.*, 2005, **43**, 717–726.
22. Giordano, M., Kansiz, M., Heraud, P., Beardall, J., Wood, B. and McNaughton, D., Fourier transform infrared spectroscopy as a novel tool to investigate changes in intracellular macromolecular pools in the marine microalga *Chaetoceros muellerii* (Bacillariophyceae). *J. Phycol.*, 2001, **37**, 271–279.
23. Murdock, J. N. and Wetzel, D. L., FTIR micro-spectroscopy enhances biological and ecological analysis of algae. *Appl. Spectrosc. Rev.*, 2009, **44**, 335–361.
24. Laurens, L. M. L. and Wolfrum, E. J., Feasibility of spectroscopic characterization of algal lipids: chemometric correlation of NIR and FTIR spectra with exogenous lipids in algal biomass. *Bioenergy Res.*, 2011, **4**, 22–35.
25. Chisti, Y., Biodiesel from microalgae. *Biotechnol. Adv.*, 2007, **25**, 294–306.
26. Liu, Z. Y., Wang, G. C. and Zhou, B. C., Effect of iron on growth and lipid accumulation in *Chlorella vulgaris*. *Bioresour. Technol.*, 2008, **99**, 4717–4722.
27. Woertz, I., Feffer, A., Lundquist, T. and Nelson, Y., Algae grown on dairy and municipal wastewater for simultaneous nutrient removal and lipid production for biofuel feedstock. *J. Environ. Eng.*, 2009, **135**, 1115–1122.
28. Chen, Y., Xiao, B., Chang, J., Fu, Y., Lv, P. and Wang, X., Synthesis of biodiesel from waste cooking oil using immobilized lipase in fixed bed reactor. *Energy Convers. Manage.*, 2009, **50**, 668–673.
29. Sigeo, D. C., Dean, A., Levado, E. and Tobin, M. J., Fourier-transform infrared spectroscopy of *Pediastrum duplex*: characterization of a micro-population isolated from a eutrophic lake. *Eur. J. Phycol.*, 2002, **37**, 19–26.
30. Beardall, J. *et al.*, A comparison of methods for detection of phosphate limitation in microalgae. *Aquat. Sci.*, 2001, **63**, 107–121.
31. Jiang, Y., Yoshida, T. and Quigg, A., Photosynthetic performance, lipid production and biomass composition in response to nitrogen limitation in marine microalgae. *Plant Physiol. Biochem.*, 2012, **54**, 70–77.
32. Dean, A. P., Nicholson, J. M. B. and Sigeo, D. C., Changing patterns of carbon allocation in lake phytoplankton: an FTIR analysis. *Hydrobiologia*, 2012, **684**, 109–127.
33. Harwati, T. U., Willke, T. and Vorlop, K. D., Characterization of the lipid accumulation in a tropical freshwater microalgae *Chlorococcum* sp. *Bioresour. Technol.*, 2012, **121**, 54–60.
34. Rodolfi, L., Zittelli, G., Bassi, N., Padovani, G., Biondi, N., Bonini, G. and Tredici, M., Microalgae for oil: strain selection, induction of lipid synthesis and outdoor mass cultivation in a low-cost photobioreactor. *Biotechnol. Bioeng.*, 2009, **102**, 100–112.
35. Tang, H., Chen, M., Garcia, M., Abunasser, N., Ng, K. and Salley, S., Culture of microalgae *Chlorella minutissima* for biodiesel feedstock production. *Biotechnol. Bioeng.*, 2011, **108**, 2280–2287.
36. Chaichalerm, S. *et al.*, Culture of microalgal strains isolated from natural habitats in Thailand in various enriched media. *Appl. Energy*, 2012, **89**, 296–302.
37. Knothe, G., Dependence of biodiesel fuel properties on the structure of fatty acid alkyl esters. *Fuel Process. Technol.*, 2005, **86**, 1059–1070.
38. Stournas, S., Lois, E. and Serdari, A., Effects of fatty acid derivatives on the ignition quality and cold flow of diesel fuel. *Energy*, 1995, **72**, 433–437.
39. Lee, J. Y., Yoo, C., Jun, S. Y., Ahn, C. Y. and Oh, H. M., Comparison of several methods for effective lipid extraction from microalgae. *Bioresour. Technol.*, 2010, **101**, 75–77.
40. Knothe, G., 'Designer' biodiesel: optimizing fatty ester composition to improve fuel properties. *Energy Fuels*, 2008, **22**, 1358–1364.

ACKNOWLEDGEMENTS. We thank Shubhadip Chakraborty and Prof. P. K. Das, IPC Department, Indian Institute of Science (IISc), Bangalore for their help in ATR-FTIR measurements. We also thank SID and Biochemistry Department, IISc for the Central facilities for FTIR and GC-MS measurements respectively. We also thank the Ministry of Environment and Forests, Government of India and IISc for financial and infrastructure support.

Received 15 October 2012; revised accepted 5 April 2013